

# Analysis of process integration and intensification of enzymatic cellulose hydrolysis in a membrane bioreactor

Q Gan,\* SJ Allen and G Taylor

School of Chemical Engineering, Queen's University of Belfast, Belfast, BT9 5AG, UK

**Abstract:** Enzymatic cellulose hydrolysis has been studied for many years, generating rich literatures and knowledge in respect to the underlying reaction mechanism, reaction kinetics, and bioreactor systems. This paper attempts to offer some additional information and new understanding of how reaction kinetics and reactor productivity can be improved in a process involving simultaneous reaction and product separation using a purpose-built membrane reactor with a single combined reaction zone and separation zone. Different operating strategies of batch, fed batch and continuous cellulose hydrolysis were investigated with intermittent or simultaneous removal of products (reducing sugars) to reduce enzyme inhibition and improve reactor productivity. The effect of continuous and selective product removal, reduced enzyme inhibition and higher enzyme concentration in retention were examined for the potential benefit in process integration and intensification in order to lower the high process cost of the enzymatic hydrolysis process, mainly due to slow reaction kinetics and expensive enzymes. A mathematical model was offered to account for the effect of selective product (reducing sugars) separation, permeate flux, reduced cellulase inhibition, dynamic structural change of the solid substrate and possible shear deactivation of the enzyme. Computer analysis was also carried out to analyse the quasi-steady state of the reaction intermediates in order to gain an insight into the reaction mechanism in simultaneous reaction and separation systems. Some original analysis and simulation of the effect of membrane separation parameters on the overall reactor performance is offered, including the effect of membrane selectivity (rejection coefficient) and flux.

© 2005 Society of Chemical Industry

**Keywords:** process integration; process intensification; cellulose hydrolysis; membrane bioreactor

## NOTATION

$A_0$	Surface area of an individual cellulose particle ( $\text{dm}^2$ )	$C_{Sx,f}, C_{Sx,per}$	Inert concentration in the feed and permeate flow respectively ( $\text{g dm}^{-3}$ )
$C_E$	Free soluble enzyme concentration ( $\text{mg dm}^{-3}$ )	$C_{S0}$	Initial total mass concentration of cellulose ( $\text{g dm}^{-3}$ )
$C_{EP}$	Concentration of enzyme–product complex ( $\text{g dm}^{-3}$ )	$d_0$	End diameter of a cylindrical cellulose particle (mm)
$C_{E*Sc}$	Concentration of enzyme–cellulose complex ( $\text{g dm}^{-3}$ )	$D_i$	Internal enzyme diffusion coefficient ( $\text{cm}^2 \text{s}^{-1}$ )
$C_{E*Sx}$	Concentration of enzyme–inert complex ( $\text{g dm}^{-3}$ )	$D_0$	Bulk phase enzyme diffusion coefficient ( $\text{cm}^2 \text{s}^{-1}$ )
$C_{E0}$	Initial enzyme concentration ( $\text{mg dm}^{-3}$ )	$f_p, f_f$	Volumetric flow rate of permeate and feed respectively ( $\text{dm}^3 \text{h}^{-1}$ )
$C_P$	Product concentration ( $\text{g dm}^{-3}$ )	$k_{Sc1}$	Rate constant of enzyme adsorption on active cellulose ( $\text{s}^{-1}$ )
$C_{P,per}$	Product concentration in the permeate flow ( $\text{g dm}^{-3}$ )	$k_{Sc2}$	Rate constant of enzyme desorption from active cellulose ( $\text{M s}^{-1}$ )
$C_{Sc}$	Concentration of active cellulose ( $\text{g dm}^{-3}$ )	$k_P$	Rate constant of product formation ( $\text{s}^{-1}$ )
$C_{Sx}$	Concentration of inert material ( $\text{g dm}^{-3}$ )	$k_{EP1}$	Forward rate constant of competitive product inhibition of enzyme ( $\text{s}^{-1}$ )
$C_{Sc,f}, C_{Sc,per}$	Cellulose concentration in the feed and permeate flow respectively ( $\text{g dm}^{-3}$ )	$k_{EP2}$	Reverse rate constant of competitive product inhibition of enzyme ( $\text{M s}^{-1}$ )

\* Correspondence to: Q Gan, School of Chemical Engineering, Queen's University of Belfast, Belfast, BT9 5AG, UK

E-mail: q.gan@qub.ac.uk

Contract/grant sponsor: European Social Funding programme

(Received 4 June 2004; revised version received 14 September 2004; accepted 4 October 2004)

Published online 14 March 2005

$k_{Sx1}$	Rate constant of enzyme adsorption on inerts ( $s^{-1}$ )
$k_{Sx2}$	Rate constant of enzyme desorption from inerts ( $M s^{-1}$ )
$L$	Length of cylindrical substrate particle (mm)
$N'_0$	Initial number of substrate solid particles per unit volume of liquid ( $dm^{-3}$ )
$r_{Sc}$	Rate of appearance of new active substrate sites ( $g dm^{-3} h^{-1}$ )
$r_{Sx}$	Rate of appearance of new inert sites ( $g dm^{-3} h^{-1}$ )
$R_P, R_{Sc}, R_{Sx}$	Membrane rejection coefficient for products, cellulose and non-reactive inert material, respectively (dimensionless)
$t$	Time (s)
$V$	Reaction volume ( $dm^{-3}$ )
$W_{S0}$	Mass of a single cellulose particle (g)
$\beta$	Surface substrate concentration coefficient ( $g dm^{-2}$ )
$\Gamma$	Shear field residence time ( $kg m^{-1} s^{-1}$ )
$\Gamma_{max}$	Maximum shear field residence time ( $kg m^{-1} s^{-1}$ )
$\rho$	Density of the cellulose particle ( $kg m^3$ )
$\sigma$	Accessibility coefficient of newly exposed substrate (dimensionless)
$\tau$	Shear stress ( $kg m^{-1} s^{-2}$ )
$\phi_{Sx}$	Inert proportion coefficient (dimensionless)

## 1 INTRODUCTION

### 1.1 Simultaneous reaction and product removal in integrated membrane bioreactor systems

In recent years the investigation of integrated biochemical processes has in many cases involved enzyme- or cell-catalysed bio-reaction in purpose-built integrated membrane reactors featuring simultaneous and continuous product removal.<sup>1</sup> The integrated operation offers potential in improving product yield and reaction kinetics, reducing enzyme inhibition, and immobilisation of enzymes in their free soluble state.<sup>2</sup> The integrated systems may have particular advantages in reactions with inhibition or equilibrium-limited conversion. Integrated membrane reactors with different configurations have also been investigated in the areas of heterogeneous bio-reactions which take place at a solid-liquid reaction interface, such as a cellulose-water interface. Ohlson *et al*<sup>3</sup> and Hagerdal *et al*<sup>4</sup> reported that the enzymatic cellulose hydrolysis rate increased four times in a membrane bioreactor compared with that obtained in a conventional batch reactor.

While integrated reaction and separation in biochemical processes offers the aforementioned potential advantages, predictive modelling of the integrated process is sometimes difficult because an integrated process normally combines continuous and discrete dynamics behaviour of reaction and separation, especially in heterogeneous enzymatic catalysis such as

enzymatic cellulose hydrolysis. The determination of an optimal operating strategy depends on the consideration of a number of inter-related factors, namely reaction rate, reaction equilibrium, transport property of enzymes, the reliability and robustness of the enzyme/cell catalyst, the degree of product inhibition, and the product separation efficiency (membrane selectivity and permeation rate).

### 1.2 Enzymatic cellulose hydrolysis

Enzymatic hydrolysis of cellulosic material to produce fermentable reducing sugar has enormous potential in meeting global food and energy demand via a biological and environmentally desirable route. However, realisation of this potential has been deterred by the high functional complexity and cost of the cellulase enzymes, which are often composed of three or four distinctive enzymes serving different catalytic functions in the cellulose hydrolysis reaction.<sup>5,6</sup> Other contentious problems include the inherent slow reaction rate and lack of an ideal reactor system to cater for the reaction taking place at a heterogeneous solid-liquid interface. Different origin and compositional as well as structural variety of cellulosic materials also means that the effectiveness of a commercially extracted microbial cellulase is often limited because of their substrate specificity for raw cellulosic materials.

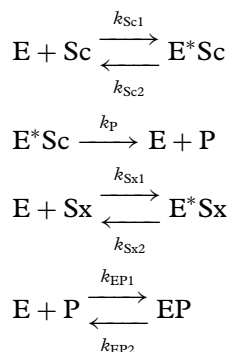
## 2 MATHEMATICAL MODELLING OF THE ENZYMATIC CELLULOSE HYDROLYSIS IN INTEGRATED REACTION AND PRODUCT SEPARATION PROCESS

Cellulosic materials are insoluble, structured, and comprised of multi-components (lignin, hemicellulose, cellulose in crystalline as well as amorphous structure, etc). Cellulose hydrolysis requires synergistic action of several cellulase components. These facts dictate that the mechanisms of enzymatic cellulose hydrolysis catalysed at the cellulose-water interface are subjected to mediation by a number of complex factors such as the structure and composition of cellulosic materials, the nature of the cellulase enzymes employed, and cellulase inhibition by intermediates (cellobios) and end product (glucose). The dynamic process of enzyme adsorption and desorption at the cellulose-water interface plays a vital role in determining the overall hydrolytic reaction rate. However, current understanding of this dynamic interaction between soluble enzyme and solid cellulose, and the interaction between cellulase and inert materials, is still limited.

In a previous analysis and mathematical modelling of the enzymatic cellulose hydrolysis in batch reactions,<sup>7</sup> we highlighted some key factors in determining the overall reaction kinetics and influence of the dynamics of the enzyme-substrate interaction in the solid-liquid two-phase reaction. These include changing substrate structure and surface composition,

accumulative loss of total enzyme activity through non-productive binding, product inhibition and shear deactivation of enzyme. In this paper, we extend the model to the simultaneous reaction and membrane separation system by incorporating new membrane filtration and separation parameters such as ultrafiltration flux, rejection coefficient and system dilution rate.

To summarise, our previously proposed model in a batch reactor featured six first order differential equations based on the reaction scheme depicted below:



In this representation,  $k_{Sc1}$  and  $k_{Sc2}$  are the primary rate constants for the formation of active  $E^*Sc$  (enzyme–cellulose) intermediate;  $k_{Sx1}$  and  $k_{Sx2}$  are the primary rate constants for the formation of non-productive  $E^*Sx$  (enzyme–inert) complex;  $k_P$  is the rate constant for product (P) formation;  $k_{EP1}$  and  $k_{EP2}$  are the forward and reverse reaction rate constants for the formation of the enzyme–product complex EP.

According to the proposed reaction scheme, the transient state concentration of the reaction intermediates  $C_{E^*Sc}$ ,  $C_{E^*Sx}$ , and  $C_{EP}$  can be expressed by three first order differential equations:

$$\frac{dC_{E^*Sc}}{dt} = k_{Sc1}C_EC_{Sc} - k_{Sc2}C_{E^*Sc} - k_PC_{E^*Sc} \quad (1)$$

$$\frac{dC_{E^*Sx}}{dt} = k_{Sx1}C_EC_{Sx} - k_{Sx2}C_{E^*Sx} \quad (2)$$

$$\frac{dC_{EP}}{dt} = k_{EP1}C_EC_P - k_{EP2}C_{EP} \quad (3)$$

In these equations,  $C_E$ ,  $C_{Sc}$ ,  $C_{Sx}$ , and  $C_P$  represent concentrations of free enzymes, digestible cellulose, inert (eg lignin) and product respectively. The rate of reducing sugar production is expressed as:

$$\frac{dC_P}{dt} = k_PC_{E^*Sc} \quad (4)$$

As the solid cellulosic material is considered to consist of an inert region and an active cellulose region, the proportional inert to total substrate ratio,  $\phi_{Sx}$ , is defined by the equation:

$$\phi_{Sx} = \frac{C_{Sx}}{C_{Sx} + C_{Sc}} = \frac{C_{Sx}}{C_{S0}} \quad (5)$$

$\phi_{Sx}$  has a similar notion to the substrate crystallinity index used by Fan *et al*<sup>8</sup> in their modelling of cellulose kinetics. The initial value of the coefficient,  $\phi_{Sx,0}$ , reflects the quality of the cellulose substrate.

As the hydrolytic reaction progresses, the first layer of cellulose substrate at the substrate–water interface is dissolved, leaving behind the inert at its original spatial co-ordinate. A new cellulose–water–enzyme reaction interface emerges as the hydrolysis moves inside the solids structure, exposing new cellulose and additional inert material which may absorb and occupy more free enzymes.

The dynamic change of the interfacial inert to total substrate ratio is taken into account in our proposed model by adding relevant terms of the emergence of cellulose and inert from inside the substrate solids structure into the following two mass balance equations for Sc and Sx:

$$\frac{dC_{Sc}}{dt} = k_{Sc2}C_{E^*Sc} - k_{Sc1}C_EC_{Sc} + r_{Sc} \quad (6)$$

$$\frac{dC_{Sx}}{dt} = k_{Sx2}C_{E^*Sx} - k_{Sx1}C_EC_{Sx} + r_{Sx} \quad (7)$$

$r_{Sc}$  and  $r_{Sx}$  represent the rate of appearance of new cellulose and inert respectively at the reaction interface.  $r_{Sc}$  and  $r_{Sx}$  can be related to the rate of reducing sugar production using the equations:

$$r_{Sc} = \sigma(1 - \phi_{Sx})\frac{dC_P}{dt} \quad (8)$$

$$r_{Sx} = \sigma\phi_{Sx}\frac{dC_P}{dt} \quad (9)$$

$\sigma$  ( $0 < \sigma < 1$ ) is the accessibility coefficient of the newly exposed substrate, which denotes the degree of accessibility of the newly exposed cellulose/inert to the enzymes. The physical significance of  $\sigma$  can be defined by the equation:

$$\sigma = \frac{D_i}{D_0} \quad (10)$$

where  $D_i$  is the internal diffusion coefficient and  $D_0$  the bulk phase diffusion coefficient.

This series of equations can be numerically analysed together with the linear enzyme conservation equation which is expressed as:

$$C_E = C_{E0} - C_{E^*Sc} - C_{E^*Sx} - C_{EP} \quad (11)$$

$C_{E0}$  is the initial total enzyme concentration (at  $t = 0$ ) and  $C_E$  the concentration of free enzyme concentration.

There has been evidence<sup>9,10</sup> to suggest that enzyme deactivation by shear stress can be related to the product of shear field strength and shear field exposure time—the *shear field residence time*  $\Gamma$ :

$$\Gamma = \tau t \quad (12)$$

where  $\tau$  is shear stress tensor and  $t$  shear exposure time.

The effect of loss of enzyme activity by shear deactivation is incorporated into our model by proportioning the active soluble enzyme ( $C_E^*$ ) as a fraction of total free soluble enzyme ( $C_E$ ) using the proportional factor  $\Gamma/\Gamma_{\max}$ .

$$C_E^* = C_E(1 - \Gamma/\Gamma_{\max}) \quad (13)$$

$$\Gamma_{\max} = \tau_{\max}t_{\max} \quad (14)$$

Equations (1)–(14) form our mechanistic model describing the reaction kinetics of enzymatic cellulose hydrolysis in a continuous batch reactor, which take into account the dynamic enzyme–cellulose, enzyme–inert and enzyme–product interactions, as well as the effect of changing substrate and enzyme deactivation by shear stress. Detailed discussion of the model for batch cellulose hydrolysis can be found in a previous study.<sup>7</sup>

In modelling the integrated membrane reactor system, modifications of eqns (4), (6) and (7) are necessary to incorporate the effect of continuous product separation from the reactor and simultaneous addition of fresh cellulosic substrate. The mass balance on product P, active cellulose Sc, and inert Sx becomes:

$$\frac{dC_P}{dt} = k_P C_{E^*S_c} - \frac{f_P C_{P,per}(1 - R_P)}{V} \quad (15)$$

$$\begin{aligned} \frac{dC_{Sc}}{dt} = & k_{Sc2} C_{E^*S_c} - k_{Sc1} C_E C_{Sc} + \sigma \frac{dC_P}{dt} + \frac{f_f C_{Sc,f}}{V} \\ & - \frac{f_P C_{Sc,per}(1 - R_{Sc})}{V} \end{aligned} \quad (16)$$

$$\begin{aligned} \frac{dC_{Sx}}{dt} = & k_{Sx2} C_{E^*S_x} - k_{Sx1} C_E C_{Sx} + \sigma \frac{\phi_{Sx}}{1 - \phi_{Sx}} \frac{dC_P}{dt} \\ & + \frac{f_f C_{Sx,f}}{V} - \frac{f_P C_{Sx,per}(1 - R_{Sx})}{V} \end{aligned} \quad (17)$$

where  $f_p, f_f$  = volumetric flow rate of permeate and feed respectively  
 $R_P, R_{Sc}, R_{Sx}$  = membrane rejection coefficient for products, cellulose and non-reactive inert material (eg hemi-cellulose and lignin)

$V$  = reaction volume

$C_{P,per}$  = product concentration in the permeate flow

$C_{Sc,f}, C_{Sc,per}$  = cellulose concentration in the feed and permeate flow respectively

$C_{Sx,f}, C_{Sx,per}$  = inert concentration in the feed and permeate flow respectively

When the reactor is operated at steady state during a continuous reaction and separation process,  $f_p = f_f$ . For the ultrafiltration membrane used in this work

the rejection coefficients  $R_{Sc} = R_{Sx} = 1$  (complete rejection of solids substrate), and  $R_P = 0$  (no rejection of reducing sugar). It is also assumed that mixing in the reactor is perfect so that  $C_{P,per} = C_P$  (product in the permeate flow has the same concentration as in the reactor). By defining the reactor dilution rate:

$$D = \frac{f_p}{V} \quad (18)$$

Equations (15), (16) and (17) can be rewritten as:

$$\frac{dC_P}{dt} = k_P C_{E^*S_c} - DC_P \quad (19)$$

$$\begin{aligned} \frac{dC_{Sc}}{dt} = & k_{Sc2} C_{E^*S_c} - k_{Sc1} C_E C_{Sc} + \sigma \frac{dC_P}{dt} \\ & + DC_{Sc,f} \end{aligned} \quad (20)$$

$$\begin{aligned} \frac{dC_{Sx}}{dt} = & k_{Sx2} C_{E^*S_x} - k_{Sx1} C_E C_{Sx} + \sigma \frac{\phi_{Sx}}{1 - \phi_{Sx}} \frac{dC_P}{dt} \\ & + DC_{Sx,f} \end{aligned} \quad (21)$$

Assuming product in the reactor and in the permeate flow has the same concentration, the production of reducing sugar in the integrated reactor operating in a simultaneous reaction and product separation mode is expressed as:

$$\text{Production} = (C_P V + C_P f_p t)/V = C_P(1 + Dt) \quad (22)$$

Knowledge of the values of the primary rate constant ( $k_{Sc1}, k_{Sc2}, k_{Sx1}, k_{Sx2}, k_P, k_{EP1}, k_{EP2}$ ) is sketchy, and methods for measuring these constants are limited due to the heterogeneous nature of the complex enzymatic catalysis at the solid–liquid interface. Assuming the primary rate constants are not affected by the operating mode of the reactor, values of the constants are adopted from literature or assumed values were used when unavailable for computer simulation of the reaction kinetics.<sup>7</sup>

### 3 EXPERIMENTAL METHODS AND MATERIALS

The cellulose substrate (Sigma C8002) used in this work is an alpha-cellulose fibre produced from hardwood pulp. The cellulose substrate particle size distribution was classified using an Endecotts octagon digital sieve shaker, showing the majority of the cellulosic substrate consisted of particles within a size range of 38–106  $\mu\text{m}$ .<sup>7</sup> All hydrolysis studies were carried out using unclassified mixed particles apart from where otherwise stated.

The reducing sugar concentration was measured using a refractor-meter (Mettler Toledo RA510M) which measures total concentration of reducing sugars in the solution based on the solution refractive index. For cross-checking and correlation, the total reducing sugar concentration was also chemically measured using the dinitrosalicylic acid (DNS) method.<sup>11</sup>

The cellulase enzymes extracted from *Trichoderma reesei* used in this work were purchased from Sigma

(Catalogue No C8546). The molecular weight of the cellulase enzymes ranges from 48 000 to 52 000 Da. All hydrolytic reactions were carried out at 40 °C, the optimal temperature of the cellulases, and temperature control was obtained by placing the integrated reactor–separator in a water bath. The reactions were conducted at a constant pH 4.7, maintained by a sodium acetate buffer.

The bench-scale reactor used in this work was fabricated from a modified Amicon dead end filtration cell (Amicon PM10) with a maximum holding volume of 2.5 dm<sup>3</sup>. A flat sheet Amicon polysulfone ultrafiltration membrane with a molecular weight cut-off (MWCO) value of 10 000 Da, a diameter of 150 mm and surface area of 0.0177 m<sup>2</sup> is installed at the base of the filtration cell. The modified reactor, situated inside a water bath for temperature control, is equipped with automatic on-line measurement of temperature, pH, feed flow rate, and membrane permeate flux. The reactor is also equipped with an agitator with a maximum agitation speed of 750 rpm to provide sufficient agitation and mixing. All permeation experiments were conducted at a transmembrane pressure (TMP) of 0.70 bar. Figure 1 shows a schematic flow diagram of the integrated reactor system.

The membrane reactor system integrates reaction and separation zone inside one device. This design allows a high degree of operating flexibility that the reactor can be operated either as a conventional batch reactor with the permeate line closed or as a continuous membrane reactor having a combined reaction and separation zone for simultaneous reaction and product separation. This design differs from most reported integrated membrane reactor systems which adopt a recycle CSTR configuration where the reaction takes place in an agitated vessel reactor and the separation takes place in a physically detached cross-flow ultrafiltration system. In this type of design, the membrane system separates the products from the substrate as well as the enzyme which is recycled back to the vessel reactor.

Measurement of reducing sugar concentration in permeate flow and inside the integrated reactor showed that the Amicon ultrafiltration membrane has a reducing sugar rejection coefficient  $R_p = 0$  (no product rejection), and substrate (cellulose particles)

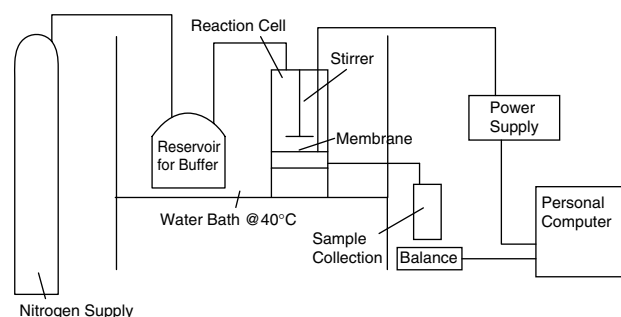


**Figure 1.** Schematic flow diagram of the integrated membrane reactor system.

rejection coefficient  $R_s = 1$  (complete rejection). The rejection coefficient for a particular component is defined as:

$$R = 1 - C_{p,i}/C_{r,i} \quad (23)$$

where  $C_{p,i}$  is the concentration of component  $i$  in permeate flow, and  $C_{r,i}$  the concentration in the reactor.

The use of the MWCO 10 000 ultrafiltration membrane allows free transmission of reducing sugars ( $R_p = 0$ ), but no transmission of enzyme molecules and solid substrate ( $R_E = 1$ ,  $R_{Sc} = 1$ ). It is also assumed that mixing in the reactor was perfect with uniform product concentration. These statements satisfy the assumption that product concentration in the permeate flow is the same as product concentration in the reactor.

#### 4 RESULTS AND DISCUSSION

The heterogeneous nature of the hydrolytic reaction with a solid substrate and soluble products catalysed by an enzyme requires related consideration in designing an operating regime for the integrated membrane reactor system. The integrated reactor with combined reaction and separation zone permits a high degree of operating flexibility to allow testing and optimising operating strategy for maximising reactor productivity and substrate conversion. In this work, three different operating strategies were investigated:

- (I) Batch reaction with continuous or intermittent product separation from the reactor with replenishment of buffer but without feeding of fresh cellulose substrate.
- (II) Fed batch operation with intermittent product separation followed by addition of fresh cellulose substrate and replenishment of buffer;
- (III) Simultaneous reaction and product separation coupled with continuous feeding of fresh cellulose and buffer.

Operating mode (III) represents the most comprehensive operating strategy of simultaneous reaction and separation. Analysis of these different operating strategies is important for maximising the productivity and yield of the reactor. It also helps to gain a better understanding of the complex underlying reaction mechanism, and the dynamics of changing substrate (cellulose) structure/composition.

##### 4.1 Batch reaction combined with continuous or intermittent product removal (operating mode I)

In operating batch cellulose hydrolysis combined with continuous product withdrawal through permeate flow, fresh buffer solution (cellulose-free) was added to the reactor at a rate running at one-tenth of the typical unrestricted permeation flow rate shown in Fig 2. The permeation flow was restricted so that reducing sugars in the permeate were not too dilute

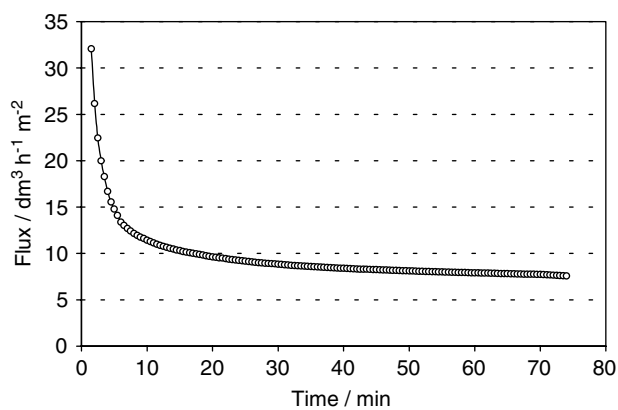


**Figure 2.** Typical flux through the Amicon ultrafiltration membrane,  $C_{S0} = 35 \text{ g dm}^{-3}$ ,  $C_{E0} = 200 \text{ mg dm}^{-3}$ ,  $T = 40^\circ\text{C}$ ,  $\text{TMP} = 0.70 \text{ bar}$ ,  $\text{pH} = 4.7$ .

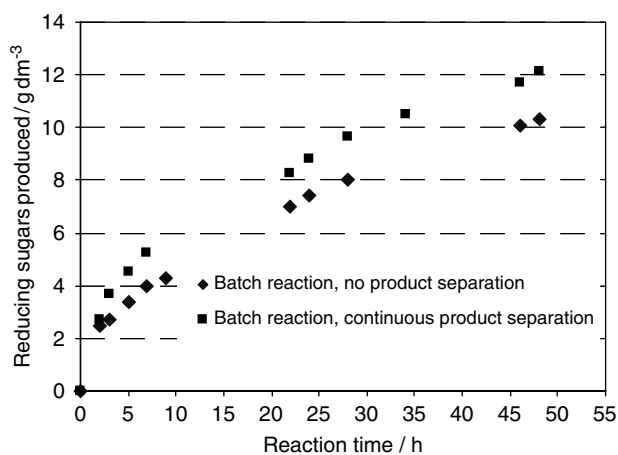


**Figure 3.** Production of reducing sugars in (i) conventional batch reaction and (ii) batch reaction combined with continuous product withdrawal through permeation.  $C_{E0} = 200 \text{ mg dm}^{-3}$ ,  $C_{S0} = 35 \text{ g dm}^{-3}$ ,  $T = 40^\circ\text{C}$ ,  $\text{TMP} = 0.70 \text{ bar}$ ,  $\text{pH} = 4.7$ .

to put excessive demand on further downstream processes (eg concentration of reducing sugars through evaporation). Addition of fresh buffer solution to the reactor was carried out at a flow rate matching the restricted permeation flow rate in order to keep the volume of the reactor constant.

Total reducing sugars production in this operation mode was compared with conventional batch reaction without continuous product separation (Fig 3), which shows that total reducing sugars production was about 20% higher after 50 h reaction. However this advantageous gain in reducing sugars production is offset by the problem of very dilute concentration of reducing sugars in the reactor and in the permeate flow, typically less than  $2.0 \text{ g dm}^{-3}$ . The large increase of total volume is somehow prohibitive for adopting this operating strategy as it put excessive demand for a further downstream evaporation process for recovery of reducing sugars.

In an attempt to overcome the problem of dilute product concentration in permeate flow, a batch cellulose hydrolysis reaction was carried out without product removal (permeation line closed) until the

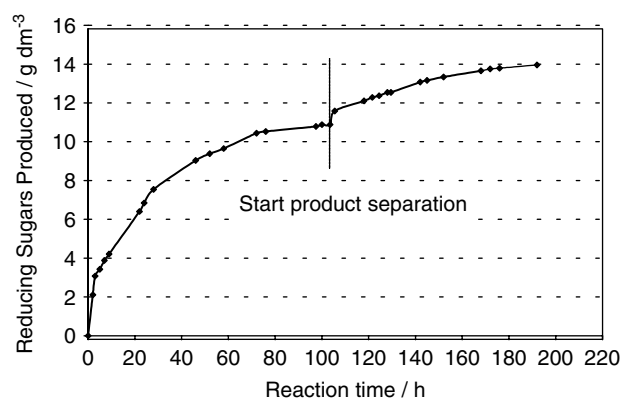


**Figure 4.** Production of reducing sugars in conventional batch reaction with one single withdrawal of permeate at 100 h.  $C_{E0} = 200 \text{ mg dm}^{-3}$ ,  $C_{S0} = 35 \text{ g dm}^{-3}$ ,  $T = 40^\circ\text{C}$ ,  $\text{TMP} = 0.70 \text{ bar}$ ,  $\text{pH} = 4.7$ .

hydrolytic reaction reached a pseudo-equilibrium state when little additional reducing sugar was produced (Fig 4). At this point, the permeation line was opened to allow a discharge of 75% of the reactor volume. The reactor was then restocked with fresh buffer solution to make up the original reactor volume, but no fresh cellulose was added. The sugar production rate increased immediately after the product was withdrawn. However this sharp rate increase was short-lived and the hydrolysis reaction reverted to the slower reaction rate of the long run.

#### 4.2 Fed batch reaction with intermittent product removal (operating mode II)

The aforementioned experiments did not deliver the desired overall improvement through the integrated reaction and separation approach as it only employed a product separation strategy without addition of new cellulose. In fed batch reaction with intermittent product removal, the reactor was initially operated under conventional batch reaction conditions to a point that the reaction reached a pseudo-equilibrium state. This was followed by a predetermined withdrawal of product from the reactor and addition of fresh cellulose.

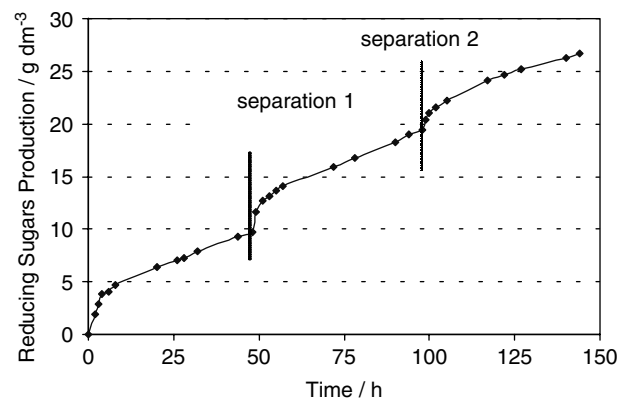


**Figure 5.** Reducing sugars production in fed batch reaction with two product removal at 48 and 96 h each followed by substrate addition of  $25 \text{ g dm}^{-3}$ ,  $C_{E0} = 200 \text{ mg dm}^{-3}$ ,  $C_{S0} = 35 \text{ g dm}^{-3}$ ,  $T = 40^\circ\text{C}$ ,  $\text{TMP} = 0.70 \text{ bar}$ ,  $\text{pH} = 4.7$ .

Figure 5 shows a typical total reducing sugar production during such an operation. The reaction was run for 48 h in the batch mode followed by a discharge of 75% of the volume of the reactor liquid phase through permeate flow. The cell was then re-stocked with buffer solution and a further 25 g fresh cellulose substrate. This separation and restocking process was repeated after a further 48 h.

Careful examination of Fig 5 shows that the reaction rate shot up immediately after the first product separation and addition of fresh cellulose. Similar to results presented in Fig 4, the increased reaction rate cannot maintain itself for more than 3 h, after which the reaction reverted to the long run rate. The same operation of permeate withdrawal and cellulose addition was repeated at 96 h. This time, the reaction rate increase was less pronounced than that at 48 h, probably caused by an accumulated loss of enzyme activity due to a combination of factors of product inhibition, shear deactivation, and increasing binding of the enzyme molecules at the non-hydrolysable region of the solid substrate as more non-reactive binding sites emerge at the solid-liquid reaction interface due to change of the solid substrate composition and structure during the long reaction.

#### 4.3 Integrated reaction and product separation with continuous substrate feeding (operating mode III)

The integrated process can be analysed in analogue to a conventional CSTR (continuous stirred tank reactor) as it also features continuous substrate feeding. The difference lies with the total absence of cellulose substrate in the reactor effluent (permeate flow). As previously stated, the perfect mixing in the reactor and zero rejection of reducing sugar by the membrane satisfy the condition that reducing sugar concentration in the effluent of the reactor is the same as that inside the reactor.

Cellulose substrate was fed to the reactor at conditions of  $f_f = 0.074 \text{ dm}^3 \text{ h}^{-1}$  and mass concentration  $C_{S,f} = 6.00 \text{ g dm}^{-3}$ , this represents a controlled steady state permeation rate of  $4.2 \text{ dm}^3 \text{ h}^{-1} \text{ m}^{-2}$  to maintain the same reaction volume in the reactor, and an addition of  $0.44 \text{ g h}^{-1}$  fresh cellulose to the reactor. Figure 6 presents the experimental results and numerical simulation of production of reducing sugars. The production is much higher and faster in this operating mode as greater substrate and enzyme loading can be facilitated to retain the expensive enzyme molecules and maintain their activity through selective product removal. In comparison to the fed batch operation (mode II), the reaction almost maintained a constant reaction rate in over 100 h of operation, indicating a more active enzyme molecule population was maintained throughout the reaction as fresh cellulose competed for free soluble enzyme molecules to prevent a more severe accumulated loss of active enzyme molecules to competing inert materials. A more effective enzyme catalysis was achieved based on

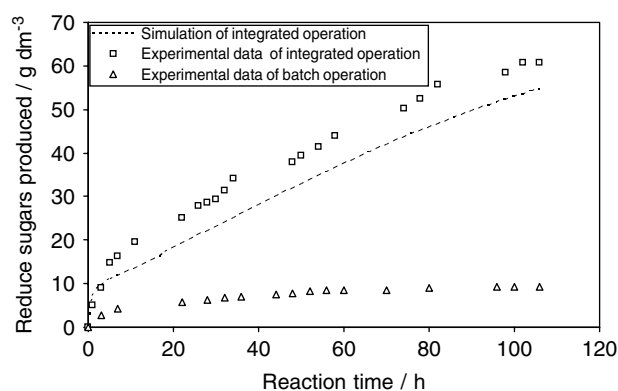


**Figure 6.** Reducing sugar production in integrated reaction with continuous product separation. Experimental and simulation conditions:  $C_{E0} = 500 \text{ mg}$ ,  $C_{S0} = 35 \text{ g}$ ,  $f_f = 0.074 \text{ dm}^3 \text{ h}^{-1}$ ,  $C_{S,f} = 6 \text{ g dm}^{-3}$ ,  $T = 40 \text{ }^\circ\text{C}$ ,  $\text{TMP} = 0.70 \text{ bar}$ ,  $\text{pH} = 4.7$ ,  $\phi_{Sx,0} = 0.10$ ,  $\beta = 0.025$ ,  $d_0 = L = 0.065 \text{ mm}$ ,  $D_0 = 1 \times 10^{-7} \text{ cm}^2 \text{ s}^{-1}$ ,  $\sigma = 0.1$ .

per unit enzyme used. The results evidently suggest that the integrated process offers a clear opportunity for process intensification at high substrate and enzyme concentration for greater reactor productivity.

The mathematical model set out in section 2 was adopted for simulation of the effect of continuous and selective separation of reducing sugars, and the effect of continuous addition of fresh solid cellulosic substrate. Since only cellulose exposed at the solid-liquid reaction interface is available for enzyme binding and catalysis, instead of using a total substrate mass concentration, we adopted a concept of effective surface concentration of active cellulose. Since the total substrate-water interfacial surface area depends on the size of substrate particles, the following two equations are used for the calculation of the initial active surface cellulose and inert material concentration:

$$C_{Sc,0} = \beta(1 - \phi_{Sx})A_0N'_0 \quad (24)$$

$$C_{Sx,0} = \beta\phi_{Sx}A_0N'_0 \quad (25)$$

$A_0$  is the surface area of an individual cellulose particle,  $N'_0$  the initial number of substrate solids particles per unit volume of liquid, and  $\beta$  the active cellulose surface concentration coefficient.  $\beta$  possesses a notion of accessible and hydrolysable cellulose substrate which possesses active enzyme binding sites on the particle surface. It distinguishes active cellulose from inert as well as non-productive crystalline cellulose and cellulose initially residing inside the solid structure which are unavailable to enzyme binding.

Assuming that the fibrous substrate particles have a uniform cylindrical form with end diameter  $d_0$  and length  $L$ ,  $N'_0$  can be calculated using the equation:

$$N'_0 = \frac{C_{S0}}{W_{S0}} = \frac{C_{S0}}{\frac{\pi d_0^2 L}{4}} \quad (26)$$

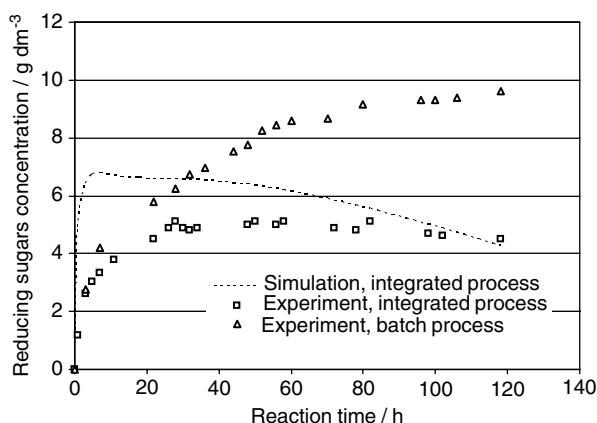


**Figure 7.** Reducing sugars concentration in the membrane reactor operated in batch and integrated reaction–separation mode. Experimental and simulation conditions:  $C_{E0} = 500$  mg,  $C_{S0} = 35$  g,  $f_f = 0.074$  dm<sup>3</sup> h<sup>-1</sup>,  $C_{Sf} = 6$  g dm<sup>-3</sup>,  $T = 40$  °C,  $TMP = 0.70$  bar,  $pH = 4.7$ ,  $\phi_{Sx,0} = 0.10$ ,  $\beta = 0.025$ ,  $d_0 = L = 0.065$  mm,  $D_0 = 1 \times 10^{-7}$  cm<sup>2</sup> s<sup>-1</sup>,  $\sigma = 0.1$ .

where  $C_{S0}$  is the initial total mass concentration of substrate,  $W_{S0}$  the weight of a single substrate particle,  $\rho$  the density of substrate particle.

The results of computer simulation (Fig 6) showed that the modified model has correctly predicted the change of reaction kinetic profile in the integrated process, with slight underestimate of the reducing sugar production.

Another reason behind a steady reaction rate in the integrated process is a lower product concentration in the reactor as it was continuously removed, thereby reducing the risk of accumulated inhibitory effect which may become irreversible. Figure 7 shows that the reducing sugar concentration in the membrane reactor fell progressively over the experimental time. The model predicted a much sharper initial increase of sugar concentration than the experimental findings, but it correctly predicted the falling trend of the sugar concentration over a longer reaction period. The discrepancy between the model prediction and the experimental data in the initial reaction stage could be caused by a higher, but faster declining, permeation rate through the membrane in the initial stage of the experiment, while a constant low steady flux was used in the model calculation.

In comparison to the batch process, the moderately lower product concentration in the integrated reactor effluent is a drawback for the integrated approach as it puts additional demand on the downstream sugar concentration process. This drawback could be partially offset as no further downstream product separation from the solid substrate residue is required in the integrated reaction and separation process. Lee and Kim<sup>12</sup> reported that a two-fold increase in glucose concentration caused a reduction of almost 40% in the rate of cellobiose hydrolysis. It is therefore required to keep glucose concentration to a minimum. This can be achieved in a membrane reactor with a low residence time, thus continually removing glucose. This, however, leads to a low glucose concentration in

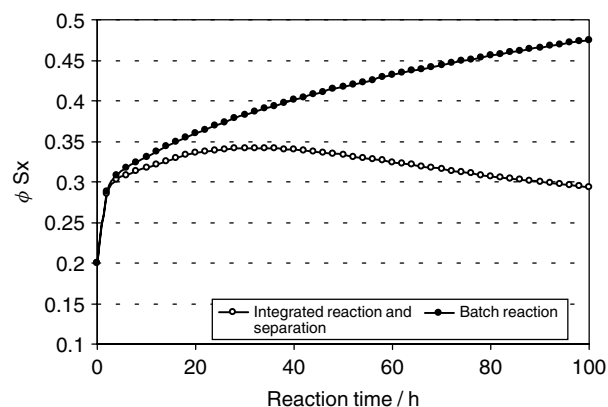


**Figure 8.** Simulation of time dependence of the inert ratio  $\phi_{Sx}$  in batch and integrated reaction–separation mode. Simulation conditions:  $C_{E0} = 500$  mg,  $C_{S0} = 35$  g,  $f_f = 0.074$  dm<sup>3</sup> h<sup>-1</sup>,  $C_{Sf} = 6$  g dm<sup>-3</sup>,  $\phi_{Sx,0} = 0.20$ ,  $\beta = 0.025$ ,  $d_0 = L = 0.065$  mm,  $D_0 = 1 \times 10^{-7}$  cm<sup>2</sup> s<sup>-1</sup>,  $\sigma = 0.1$ .

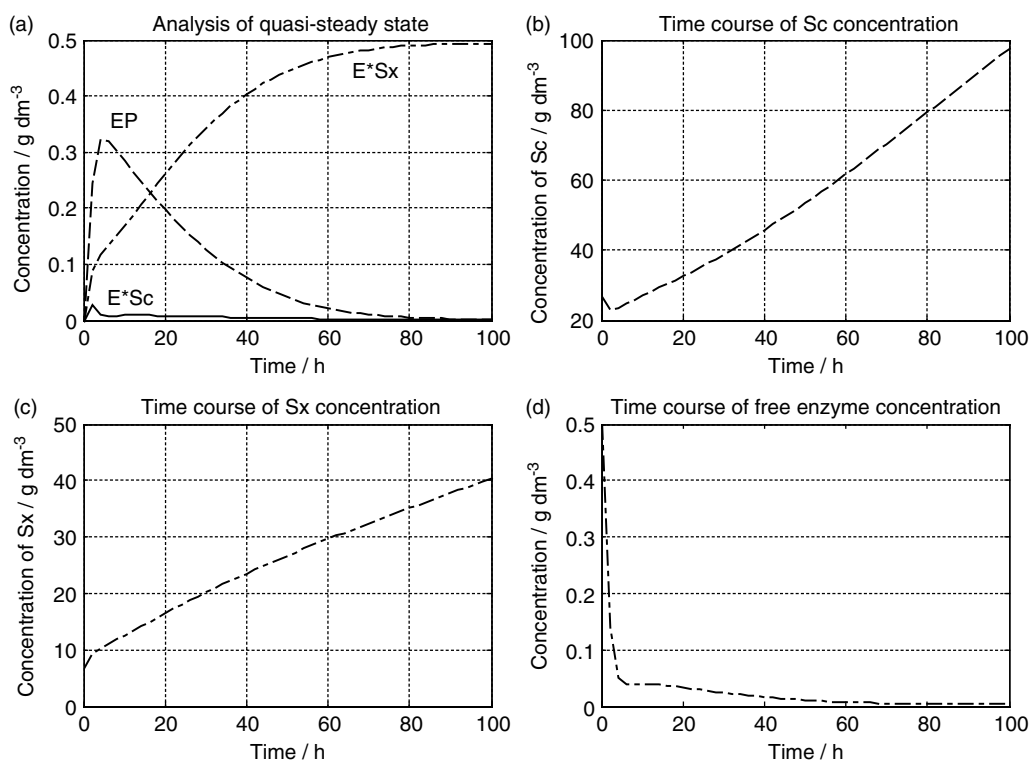
the filtrate, which would have to be concentrated for further industrial applications.

Figure 8 shows model simulation of the dynamic change of the inert to total substrate ratio,  $\phi_{Sx}$ , in the integrated process. The significant rate-reducing effect of dynamic change of substrate quality and non-productive enzyme binding on the inert has been underestimated in many studies. The simulation results indicate that the initial increase of  $\phi_{Sx}$  is rapid, mainly because of a high concentration of free soluble enzyme and fast reaction rate. The increase in the  $\phi_{Sx}$  value gradually petered out, as the reaction rate fell and the additional supply of fresh substrate restrained the further increase in  $\phi_{Sx}$  value. This hypothesis, though speculative in nature and difficult to validate by experiments, provides a plausible explanation for the different reaction kinetics in batch reactors and the integrated reactor system.

#### 4.4 Analysis of quasi-steady state

To obtain an insight of the reaction course and transient state component (Sc, Sx and E) concentration, and to examine a possible existence of a quasi-steady state for the formation of enzyme–substrate (E\*Sc and E\*Sx) and enzyme–product (EP) complex, a computer simulation was carried out for the time course of concentrations of the components in both integrated reaction/separation operation (Fig 9) and conventional batch reaction without simultaneous product separation (Fig 10). The theories described in the following paragraphs, with a degree of speculation based on results from computer simulation of the proposed reaction scheme and kinetic modelling, provide an interesting insight into the complex transient state of the two-phase reaction mediated by enzymes at the solid–liquid interface.

The simulation results suggested the existence of a quasi-steady state for the E\*Sc complex in both operation modes (Figs 9(a), 10(a)), and a continuous increase of E\*Sx concentration which may explain the cause of a continuous reduction of apparent enzyme



**Figure 9.** Simulation of the quasi-steady state (a) and the time course of concentrations of active cellulose (b), non-reactive inert (c), and free soluble enzymes (d) in integrated reaction–separation mode. Simulation conditions:  $C_{E0} = 500$  mg,  $C_{S0} = 35$  g,  $f_t = 0.074$  dm<sup>3</sup> h<sup>-1</sup>,  $C_{Sf} = 6$  g dm<sup>-3</sup>,  $\phi_{Sx,0} = 0.20$ ,  $\beta = 0.025$ ,  $d_0 = L = 0.065$  mm,  $D_0 = 1 \times 10^{-7}$  cm<sup>2</sup> s<sup>-1</sup>,  $\sigma = 0.1$ .

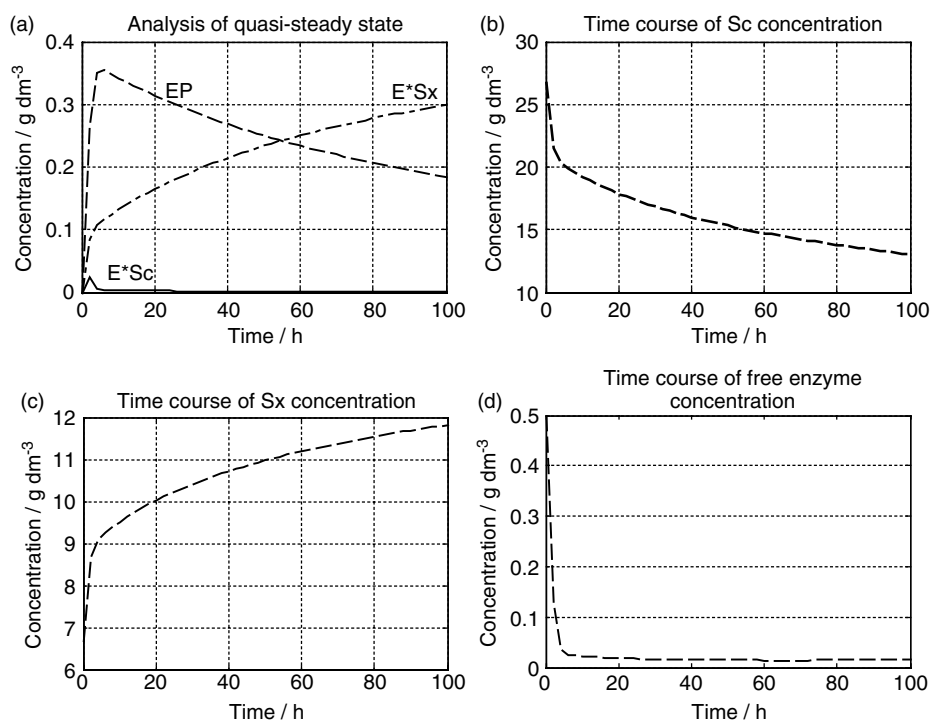


**Figure 10.** Simulation of the quasi-steady state (a) and the time course of concentrations of active cellulose (b), non-reactive inert (c), and free soluble enzymes (d) in conventional batch reaction. Simulation conditions:  $C_{E0} = 500$  mg,  $C_{S0} = 35$  g,  $\phi_{Sx,0} = 0.20$ ,  $\beta = 0.025$ ,  $d_0 = L = 0.065$  mm,  $D_0 = 1 \times 10^{-7}$  cm<sup>2</sup> s<sup>-1</sup>,  $\sigma = 0.1$ .

activity. The formation of the EP complex, which is reversible, also showed a strong dependence on reaction time.

The concentration of active cellulose ( $C_{Sc}$ ) decreased rapidly with time in the first few hours

in the batch reaction (Fig 9(b)). The concentration of Sc also decreased in the integrated operation in at the beginning of the reaction (Fig 10(b)), but turned higher as the supply rate of fresh substrate overtook the reaction rate which decreased rapidly in the first

few hours. Concentration of  $S_x$  increased with time in both operation modes (Figs 9(c), 10(c)), indicating a change of substrate composition and likely also a change of structure along with the progress of the hydrolytic reaction.

In both operation modes, the concentration of free soluble enzyme (E) decreased rapidly before the reactions reached a relatively steady state (Figs 9(d), 10(d)). This suggests a very dynamic enzyme–substrate and enzyme–product interaction at the beginning of the reaction, which resulted in a rapid loss of free enzyme molecules to the formation of the intermediate complexes. After the initial stage, the free enzyme concentration remained at a very low level, but the production of reducing sugar maintained a relative steady rate for over 100 h (Fig 6). It is not clear why the steady reaction rate has lasted so long when the free enzyme concentration has decreased dramatically. One possible reason could be the gradual and reversible dissociation of the EP complex to release more products, i.e. the rapid build-up of EP complex at the initial stage of the reaction acted as a reservoir for the later stage production of reducing sugars.

## 5 FURTHER DISCUSSION AND CONCLUSION

By employing an intermittent product separation strategy in both batch and fed batch mode (operating modes I and II), we have observed a rather limited improvement in reducing sugar productivity in the integrated reactor system. The usefulness of combined product separation and reaction in these operations is limited by the inherent slow reaction rate and the complex and heterogeneous nature of the enzymatic reaction. The effect of some key factors such as cellulose inhibition and dynamic change of solid substrate structure on the reaction rate and the overall conversion ratio in batch cellulose hydrolysis have been extensively reported,<sup>7,13,14</sup> and these factors also have crucial influence on the effectiveness of the simultaneous reaction and separation operating strategy. Two factors may have played particularly important roles in limiting the overall success of the integrated operation:

- (i) Enzyme binding onto inert materials (eg lignin or hardly hydrolysable crystalline cellulose) may progressively become a dominant factor in causing loss of overall enzyme activity, and unlike product inhibition which can be reduced through removal of reducing sugars, the inert binding progresses with reaction as the solids–liquid reaction interface was gradually stripped of cellulose and the solids' surface became saturated with the inert. Mass transfer limitation may also reduce the accessibility of active cellulose residing inside the solids substrate:
- (ii) The remaining free soluble enzyme molecules may progressively lose activity because of shear deactivation inside the agitated reactor, the effect

of which accumulates with prolonged shear field residence time.

Despite limited success of simultaneous product separation strategy in the aforementioned two operations, continuous product separation coupled with continuous feeding of fresh cellulose substrate (operating mode III) produced remarkable improvement of the productivity of the integrated reactor. There are more likely a combination of factors contributing to the success of this operation rather than a single contribution of reduced product inhibition of the enzyme. One of the main factors could be a continuous high level of accessibility of fresh cellulose at the solid–liquid reaction interface, and low level of reducing sugar concentration in the reactor. The success of this fully integrated operation provides an opportunity for process intensification in which operation under high concentration of enzymes and substrate could be advantageous as the high concentration of enzyme molecules and overall catalytic activity would not be lost quickly, as in batch operations.

The analysis of the quasi-steady state provided some insight into how the integrated operating strategy worked during the transient and steady state. The overall analysis offers somehow a different view from some reported investigations<sup>3,4</sup> of the application of an integrated membrane reactor system in enzymatic cellulose hydrolysis. Our analysis suggests that the potential advantages of an integrated reaction and separation process is in general harder to realise in the heterogeneous enzymatic catalysis which has a slow reaction rate and involves complex enzyme–substrate interactions at the solid–liquid reaction interface.

A potential gain from applying such an integrated reaction and product separation approach could be derived from adopting a highly intensive process with greater substrate and enzyme concentrations. This approach may otherwise be denied to the conventional batch operation due to rapid loss of enzyme activity because of product inhibition in a solution of high product concentration. However this strategy may be limited to a degree by the stability and robustness of the enzyme in a more intensive mixing field.

The mathematical modelling offered in this work attempts to take account of the more dynamic and interwoven events in the complex enzymatic adsorption, catalysis, and product inhibition process. The model is considered somewhat more qualitative in respect to insufficient understanding of the dynamic enzyme adsorption and desorption process, and also in specific lack of detailed account of the synergistic actions of different cellulase components (eg endo-1,4- $\beta$ -glucanase, exo-1,4- $\beta$ -glucanase, exo-1,4- $\beta$ -glucosidase, and  $\beta$ -glucosidase). Incorporation of the varying effect of different cellulase components in a mathematical modelling with insufficient understanding of the catalytic and kinetic function of each component would inevitably lead to over-complexity and unreliability in the mathematical description. Nonetheless, this model offers a more comprehensive

approach to the understanding of reaction kinetics in integrated reaction–separation membrane systems involving two-phase solid–liquid enzymatic catalysis since it takes account of simultaneous effects of separation mass transport properties, the dynamic change of solid substrate quality, and the loss of enzymatic activity due to both product inhibition and enzyme adsorption on non-hydrolytic inert materials. Future studies would include the examination of the influence of the operating parameters of the membrane system, such as the effect of dilution rate on productivity of the reactor based on intensified reactions.

## ACKNOWLEDGEMENT

We thank the European Social Funding programme for providing a scholarship to Graeme Taylor for this project.

## REFERENCES

- 1 Chekhova E, Barton PI and Gorak A, Optimal operation processes of discrete-continuous biochemical processes. *Computers and Chemical Engineering* **24**:1167–1173 (2000).
- 2 Cauwenberg V, Vergossen P, Stankiewicz A and Kierkels H, Integration of reaction and separation in manufacturing of pharmaceuticals: membrane-mediated production of S-ibuprofen. *Chemical Eng Sci* **54**:1473–1477 (1999).
- 3 Ohlson I, Tragardh G and Hagerdel BH, Enzymatic hydrolysis of sodium-hydroxide-pretreated sawlog in an ultrafiltration membrane reactor. *Biotechnol Bioeng* **26**:647–653 (1984).
- 4 Hagerdal BH, Andersson E, Leiva ML and Mattiasson B, Membrane biotechnology, co-immobilisation, and aqueous two-phase system: alternatives in bioconversion of cellulose. *Biotechnol Bioeng Symp* **11**:651–661 (1981).
- 5 Klyosov AA and Rabinowitch ML, Enzymatic conversion of cellulose to glucose: present state of the art and potential, in *Enzyme Engineering, Future Directions*, ed by Wingard LB Jr, Berezin IV and Klyosov AA. Plenum Press, New York, pp 83–165 (1980).
- 6 Brown RF and Holtzapfel MT, A comparison of the Michaelis–Menten and HCH-1 models. *Biotechnol Bioeng* **36**:1151–1154 (1990).
- 7 Gan Q, Allen SJ and Taylor G, Kinetic dynamics in heterogeneous enzymatic hydrolysis of cellulose: an overview, an experimental study and mathematical modelling. *Process Biochemistry* **38**:1003–1018 (2003).
- 8 Fan LT, Lee YH and Beardmore DH, Major chemical and physical features of cellulosic materials as substrates for enzymatic hydrolysis. *Advances in Biochemical Engineering* **14**:101–117 (1980).
- 9 Bowen WR and Gan Q, Properties of microfiltration membranes: the effect of adsorption and shear on the recovery of an enzyme. *Biotechnol Bioeng* **40**:491–497 (1992).
- 10 Charm SE and Wang BL, Enzyme inactivation with shearing. *Biotechnol Bioeng* **12**:1103–1109 (1970).
- 11 Miller GL, Use of dinitrosalicylic acid reagent for determination of reducing sugar. *Analytical Chemistry* **31**:426–428 (1959).
- 12 Lee SG and Kim HS, Optimal operating policy of the ultrafiltration membrane bioreactor for enzymatic hydrolysis of cellulose. *Biotechnol Bioeng* **42**:737–746 (1993).
- 13 Gregg DJ and Saddler JN, Factors affecting cellulose hydrolysis and the potential of enzyme recycle to enhance the efficiency of an integrated wood to ethanol process. *Biotechnol Bioeng* **51**:375–383 (1996).
- 14 Sun Y and Cheng JY, Hydrolysis of lignocellulosic materials for ethanol production: a review. *Bioresource Technology* **83**:1–11 (2002).